Received: 09 April 2023 | Revised: 22 May 2023 | Accepted: 28 May 2023
DOI: 10.22034/ecc.2023.396611.1639
Eurasian Chemical Communications
SAMI

FULL PAPER

In silico study of chalcones having novel zinc binding group (3-propoxy-1, 2-diol) for histone deacetylase inhibitory effect

Ahmed Abdulwahid Sadon[a,*] |Shihab Hattab Mutlag[b] |Raheem Jameel Mohaisen[c]

[a]*Department of Pharmaceutical Chemistry, College of Pharmacy, University of Baghdad, Baghdad, Iraq*

[b]*Department of Pharmacology and Toxicology, College of Pharmacy, University of Baghdad, Baghdad, Iraq*

[c]*Department of Pharmaceutical Chemistry, College of Pharmacy, University of Basrah, Basrah, Iraq*

***Corresponding Author:**
Ahmed Abdulwahid Sadon
E-mail: ahmedsadon844@gmail.com
Tel.: +009647705556702

To conduct an analysis of the recently synthesized chalcone derivatives (A7-A17), the spectroscopic methods of FTIR, ^{1}H-NMR, ^{13}C-NMR, and Elemental analysis were used. An MTT test was performed to investigate the cytotoxic effects of these compounds on five unique human cancer cell lines (HepG2, MCF-7, HeLa, Ovcar-3, and A549) to identify whether or not these compounds had cytotoxic properties. Throughout the whole of this investigation, the drug adriamycin served in the role of the study's positive control medicine. In a similar fashion, *in vitro* testing with the DPPH moiety was carried out with the objective of assessing the antioxidative capacity of chalcone derivatives. The AutoDock Vina approach was used to dock the created compounds (A7-A16) and related chalcone derivatives (A1-A6), synthesized previously against the active site of *Aquifex aeolicus* histone deacetylase (HDAC) homolog, where this homolog across 375 residues exhibits a 35.2% identity with human HDAC1. According to the findings of a molecular docking study, it was shown that all of the compounds (A1-A16) exhibited a binding mode with the active site of the *Aquifex aeolicus* HDAC homolog that was extremely similar to the co-crystallized ligand (Vorinostat SAHA). This was found to be the case when the ligand was crystallized along with the HDAC homolog. The *in silico* absorption, distribution, metabolism, excretion, and toxicity (ADMET) measurements were derived to show that all ligands have acceptable pharmacokinetic properties.

KEYWORDS

Molecular docking; aquifex aeolicus histone deacetylase homolog; vorinostat SAHA; MTT assay; ADMET study.

Introduction

The term "cancer" is used to describe a collection of diseases that are defined by malignant cellular proliferation, which may lead to metastasis (the spread of the disease to other regions of the body) [1]. The cytotoxic effects of chemotherapy on healthy cells are a possible cause of the severe side effects experienced by those undergoing treatment for cancer [2].

Therefore, there is an immediate and pressing need to discover novel chemotherapeutic medications that are more selective for cancer cells and have fewer adverse side effects [3]. On the other hand, the human body is a consistent generator of

species of reactive oxygen and free radicals owing to the great diversity of continuous biological processes inside it [4].

The ability of antioxidants to scavenge free radicals, reduce oxidative stress, and slow down aberrant cell growth is directly linked to the cancer-preventing benefits of the antioxidants [5-7]. It is preferable to provide a single molecule with many mechanisms of action rather than a mixture of drugs [8]. As a result, various researchers have looked into the anticancer and antioxidant properties of newly created compounds [9-11].

Covalent chemical modifications of DNA and covalent post-translational modifications (PTMs) of histones are two examples of epigenetic controls that play an important role in gene regulation. Both of these types of modifications are examples of epigenetic controls [12]. Histone acetylation is a kind of post-translational modification (PTM), and it is reversible thanks to enzymes known as histone deacetylases (HDACs). Both histone acetyltransferases (HATs) and HDACs aim their activity at the lysine residues that are located in the histone core tail. DNA, which has a negative charge, creates strong connections with the positively charged histones, where the ε-amine of the lysine is responsible for. These interactions are necessary for the proper functioning of the cell. The acetylation of histones lowers the electrostatic potential of the lysine residues at the N^{ε}-terminus, which transforms dense heterochromatin into more open euchromatin [13].

During the DNA transcription, euchromatin should be initially unraveled so that RNA polymerase and the proteins that control gene expression can attach to the DNA. HDACs are not only engaged in regulating the acetylation of histones, but also of tubulin, p21, and p53, suggesting that they play a role in a wider range of cellular activities [14,15]. Overexpression of HDACs has been linked to many different illnesses, including inflammatory diseases, neurodegenerative disorders, and many forms of cancer [16-18].

Therefore, HDAC inhibitors may find use in medical settings. Inhibitors of HDACs typically have a three-group chemical structure. Three parts make up the HDAC inhibitor: a hydrophobic cap that interacts with the enzyme's surface rim and identifies the HDAC isoform; a zinc binding group (ZBG) composed of hydroxamate, benzamide, and thiol motifs that chelate the zinc ion at the base of the catalytic domain; and a hydrophobic carbon chain linker connecting the ZBG and the cap and spanning into the tunnel of enzyme cavity. All of these components are necessary for the enzyme to be active [19-22].

In addition, chalcones are a favored structural class with several biological functions, including antimicrobial activity [23], anti-malarial [24], anti-fungal [25], anti-Alzheimer's disease [26], anti-platelet [27], anti-oxidant [28], anti-inflammatory [29, 30], and anti-cancer activities [31-34]. HDAC inhibitors with the diol (ZBG) have been reported, like catechol derivatives (**1**) (Figure 1), which had 20.7±4.0% HeLa cell line inhibition at 100 μM compared to Trichostatin A having IC_{50}=0.0106±0.0027 μM at the same condition [35]. Catechol (**2**) (Figure 1) had an HDAC4 IC_{50} value of (24.7 μM)**,** while (**3**) (Figure 1) had an HDAC4 IC_{50} value of (4.47 μM) exhibiting much higher activity compared to SAHA (IC_{50} > 40 μM) [36], as depicted in Figure 1.

Among the natural chalcones, Butein (**4**) (Figure 1) appeared to be the best inhibitor of HDAC activity showing IC_{50} total HDAC value (60 μM) compared to (0.14 μM) of SAHA [37]. Chalcone derivative (**5**) (Figure 1) bearing the hydroxamate group as the zinc binding group showed IC_{50} (μM) of 0.62±0.04, 2.05±0.48, and 2.92±0.52 compared to 3.33±0.74, 2.18±0.35, and 1.23±0.08 of SAHA against human HepG2, MCF-7, and HCT-116 cells, respectively [38].

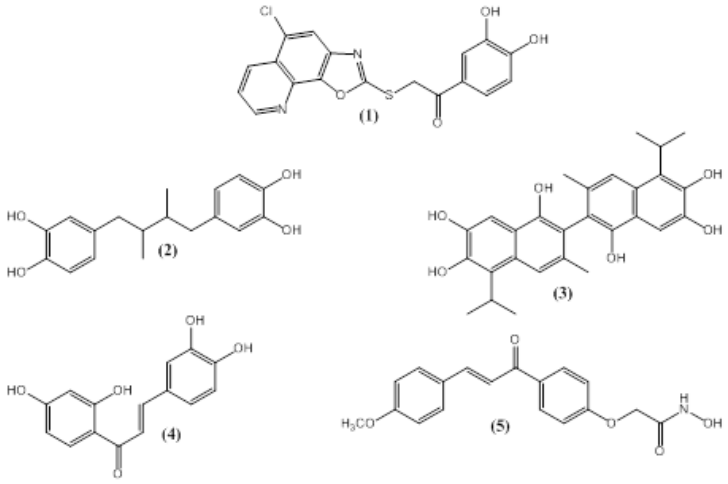

FIGURE 1 Diol and chalcone derivatives as HDAC inhibitors

According to the studies mentioned earlier, the present work aimed at gathering the two bioactive entities (chalcone) and (3-propoxy-1, 2-diol as (ZBG and antioxidant motif)) in one compact structure to increase predicted anti-tumor action. Starting from compound (5), a (chalcone with hydroxamate methoxy group), we plan to design chalcones with diol methoxy group as *novel ZBG*. The hybrids of HDACIs and chalcones (A1-A6) [39] were synthesized and assessed for their *in vitro* cytotoxic activity using an MTT-based assay against five human cancer cell lines HepG2, A549, HeLa, Ovcar-3, and MCF-7, and for DPPH radical scavenging assay to determine antioxidant activity. Other HDACIs/chalcone hybrids (A7-A16) have been synthesized and assessed for the above *in vitro* cytotoxic and antioxidant activity. HDACIs/chalcone hybrids (A1-A16) have been docked into the binding sites of *Aquifex aeolicus* histone deacetylase homolog to investigate how well they pair with the targeted binding pockets in addition to *the in silico* Absorption, Distribution, Metabolism, Excretion, and Toxicity (ADMET) study.

Experimental

Chemicals and instruments

Reagents and chemicals procured from international suppliers for use in the synthesis of chalcone derivatives. There was no additional purification on the acquired biological and chemical agents. Without any pre-correction, melting points were determined using Stuart's SMP3 melting temperature instrument. Thin-layer chromatography was utilized to test for impurities in the synthesized derivatives and track their development during the synthesis. This method uses a TLC plate supported by aluminum and coated with a silica gel 60 F_{254} sheet, as well as a mobile phase composed of a combination of n-Hexane, Ethylacetate, and Methanol (3:3:1).

The IR spectrum was collected using an ATR-FTIR spectrophotometer (Schimadzu, Japan), and the ^{13}C-NMR and ^{1}H-NMR spectra were collected in deuterated dimethyl sulfoxide (DMSO-d_6) on Inova 125 and 500 MHz instruments, respectively. Chemical shifts were recorded in parts per million, or ppm, units. The elemental analyzer, Euro EA3000, was routinely used for CHNS(O) micro-analysis.

Chemical pathways

Compound **(I)** 4-(2,3-dihydroxypropoxy)-3-methylbenzaldehyde was produced using the procedure that was explained by Ahmed *et al.* [39] (65 % yield) (m.p.: 94-96 °C). R_f = 0.35.

A general procedure for the synthesis of (chalcones A7-A16) [40-43]

10 New chalcones (A7-A16), in addition to the previously prepared (A1-A6) [39], have been synthesized as follow: one mmol (0.21 g) of (**I**) and 5 mL of ethanol was used dissolve it (except for A14 (50 mL), A15 (25 mL), and A13, A16 (15 mL), and then 0.5 mL of a 40% NaOH solution was added drop wise while continuously rotation the mixture for ten minutes at 0 ˚C.

After adding one mmol of the substituted acetophenone derivative to the mixture, the reaction was carried out while the mixture was stirred for twenty-four hours at room temperature. After observing the reaction using TLC, the mixture was then diluted with 5 mL of water and placed in the refrigerator for the duration of the night. To get pure chalcone, the precipitate was initially filtered, and then cold water was used to clean it for several times, and finally ethanol was used to recrystallize it.

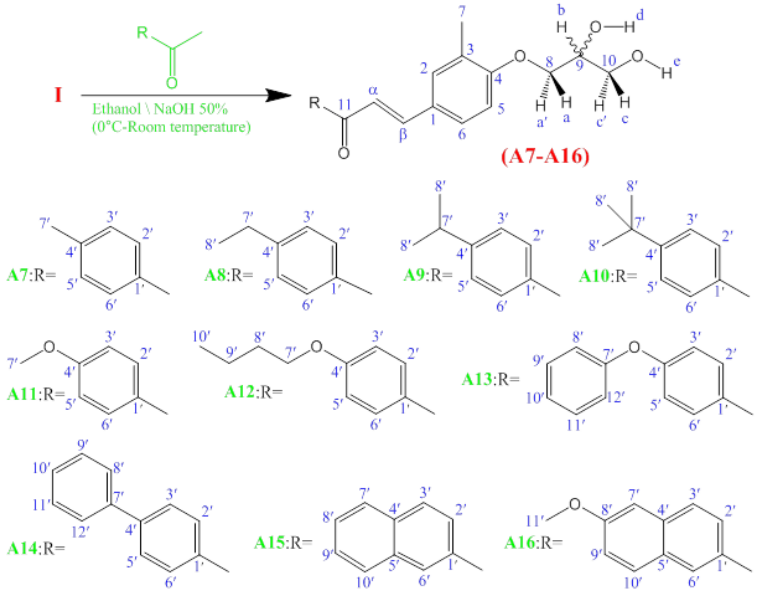

EQUATION 1 The synthesis of chalcones derivatives (**A7-A16**)

3-(4-(2,3-Dihydroxypropoxy)-3-methylphenyl)-1-(p-tolyl)prop-2-en-1-one (A7):

Yellow powder 0.189 g (58 % yield) (m.p.: 150-152 ˚C). R_f = 0.52; IR ν_{max} (cm^{-1}): 3417 (OH), 1651 (C=O); ^{1}H-NMR (ppm, 500 MHz, DMSO-d_6): δ= 7.97 (d, 3H, 2′, 6′, β), 7.46 (m, 3H, 2, 6, α), 7.25 (d, 2H, 3′, 5′), 6.74 (d, 1H, 5), 4.83 (s, 1H, d), 4.61 (s, 1H, e), 3.83 (m, 1H, b), 3.72 (m, 2H, a, a′), 3.43 (m, 2H, c, c′), 2.45 (s, 3H, 7′), and 2.09 (s, 3H, 7); ^{13}C-NMR (ppm, 125 MHz, DMSO-d_6): δ= 190.2 (11), 157.7 (4), 144.5 (β, 4′), 134.1 (1′), 131.5 (2), 129.5 (1, 2′, 3′, 5′, 6′), 128.2 (6), 127.2 (3), 122.4 (α), 113.4 (5), 70.9 (8, 9), 64.3 (10), 23.1 (7′), and 16.1 (7). Elemental analysis for $C_{20}H_{22}O_4$: C, 73.60%; H, 6.79%; O, 19.61%. Found: C, 73.56%; H, 6.89%; and O, 19.49%.

3-(4-(2,3-Dihydroxypropoxy)-3-methylphenyl)-1-(4-ethylphenyl)prop-2-en-1-one (A8):

Off white powder 0.194 g (57 % yield) (m.p.: 155-157 ˚C). R_f = 0.52; IR ν_{max} (cm^{-1}): 3286 (OH), 1652 (C=O); ^{1}H-NMR (ppm, 500 MHz, DMSO-d_6): δ= 7.95 (d, 3H, 2′, 6′, β), 7.44 (m, 3H, 2, 6, α), 7.22 (d, 2H, 3′, 5′), 6.75 (d, 1H, 5), 4.84 (s, 1H, d), 4.63 (s, 1H, e), 3.85 (m, 1H, b), 3.70 (m, 2H, a, a′), 3.41 (m, 2H, c, c′), 2.69 (q, 2H, 7′), 2.08 (s, 3H, 7), and 1.25 (t, 3H, 8′); ^{13}C-NMR (ppm, 125 MHz, DMSO-d_6): δ= 189.7 (11), 158.7 (4), 148.5 (4′), 145.5 (β), 136.1

(1′), 131.3 (2), 129.2 (1, 2′, 3′, 5′, 6′), 128.0 (6), 127.1 (3), 121.4 (α), 113.8 (5), 70.8 (8, 9), 64.1 (10), 27.5 (7′), and 15.8 (7, 8′). Elemental analysis for $C_{21}H_{24}O_4$: C, 74.09%; H, 7.11%; and O, 18.80%. Found: C, 74.29%; H, 7.17%; and O, 18.84%.

3-(4-(2,3-Dihydroxypropoxy)-3-methylphenyl)-1-(4-isopropylphenyl)prop-2-en-1-one (A9):

Off white powder 0.205 g (58 % yield) (m.p.: 155-157 ˚C). R_f = 0.55; IR ν_{max} (cm^{-1}): 3275 (OH), 1653 (C=O); ^{1}H-NMR (ppm, 500 MHz, DMSO-d_6): δ= 7.93 (d, 3H, 2′, 6′, β), 7.43 (m, 3H, 2, 6, α), 7.21 (d, 2H, 3′, 5′), 6.75 (d, 1H, 5), 4.84 (s, 1H, d), 4.62 (s, 1H, e), 3.86 (m, 1H, b), 3.75 (m, 2H, a, a′), 3.45 (m, 2H, c, c′), 2.98 (m, 1H, 7′), 2.11 (s, 3H, 7), and 1.28 (d, 6H, 8′); ^{13}C-NMR (ppm, 125 MHz, DMSO-d_6): δ= 190.4 (11), 157.7 (4), 150.5 (4′),145.5 (β), 136.1 (1′), 131.4 (2), 129.7 (1, 2′, 6′), 128.5 (6), 127.4 (3), 125.5 (3′, 5′), 121.9 (α), 114.2 (5), 70.8 (8, 9), 64.1 (10), 34.4 (7′), 23.5 (8′), and 16.1 (7). Elemental analysis for $C_{22}H_{26}O_4$: C, 74.55%; H, 7.39%; and O, 18.06%. Found: C, 74.45%; H, 7.47%, and O, 17.94%.

1-(4-(Tert-butyl)phenyl)-3-(4-(2,3-dihydroxypropoxy)-3-methylphenyl)prop-2-en-1-one (A10):

Faint yellow powder 0.214 g (58 % yield) (m.p.: 158-160 ˚C). R_f = 0.57; IR ν_{max} (cm^{-1}): 3286 (OH), 1668 (C=O); ^{1}H-NMR (ppm, 500 MHz, DMSO-d_6): δ= 7.92 (d, 3H, 2′, 6′, β), 7.42 (m, 3H, 2, 6, α), 7.21 (d, 2H, 3′, 5′), 6.76 (d, 1H, 5), 4.81 (s, 1H, d), 4.65 (s, 1H, e), 3.82 (m, 1H, b), 3.70 (m, 2H, a, a′), 3.41 (m, 2H, c, c′), 2.10 (s, 3H, 7), and 1.35 (s, 9H, 8′); ^{13}C-NMR (ppm, 125 MHz, DMSO-d_6): δ= 190.4 (11), 158.1 (4), 155.7 (4′), 145.2 (β), 137.1 (1′), 131.5 (2), 129.3 (1, 2′, 6′), 128.3 (6), 127.0 (3), 126.1 (3′, 5′), 121.8 (α), 112.9 (5), 70.6 (8, 9), 64.7 (10), 35.1 (7′), 31.0 (8′), and 15.9 (7). Elemental analysis for $C_{23}H_{28}O_4$: C, 74.97%; H, 7.66%; and O, 17.37%. Found: C, 75.01%; H, 7.60%; and O, 17.45%.

3-(4-(2,3-Dihydroxypropoxy)-3-methylphenyl)-1-(4-methoxyphenyl)prop-2-en-1-one (A11):

Beige powder 0.195 g (57 % yield) (m.p.: 166-168 ˚C). R_f = 0.48; IR ν_{max} (cm^{-1}): 3282 (OH), 1653 (C=O); ^{1}H-NMR (ppm, 500 MHz, DMSO-d_6): δ= 7.99 (d, 3H, 2′, 6′, β), 7.41 (m, 3H, 2, 6, α), 7.05 (d, 2H, 3′, 5′), 6.77 (d, 1H, 5), 4.81 (s, 1H, d), 4.64 (s, 1H, e), 3.84 (m, 4H, b, 7′), 3.75 (m, 2H, a, a′), 3.45 (m, 2H, c, c′), and 2.11 (s, 3H, 7); ^{13}C-NMR (ppm, 125 MHz, DMSO-d_6): δ= 190.5 (11), 164.1 (4′), 158.2 (4), 145.2 (β), 134.7 (1′), 131.9 (2, 2′, 6′), 129.6 (1), 128.5 (6), 127.4 (3), 121.9 (α), 113.8 (5, 3′, 5′), 71.2 (8, 9), 63.8 (10), 55.4 (7′), and 16.2 (7). Elemental analysis for $C_{20}H_{22}O_5$: C, 70.16%; H, 6.48%; and O, 23.36%. Found: C, 70.22%; H, 6.34%; and O, 23.32%.

1-(4-Butoxyphenyl)-3-(4-(2, 3-dihydroxypropoxy)-3-methylphenyl)prop-2-en-1-one (A12):

Yellow powder 0.215 g (56 % yield) (m.p.: 176-178 ˚C). R_f = 0.51; IR ν_{max} (cm^{-1}): 3421 (OH), 1644 (C=O); ^{1}H-NMR (ppm, 500 MHz, DMSO-d_6): δ= 7.97 (d, 3H, 2′, 6′, β), 7.44 (m, 3H, 2, 6, α), 7.04 (d, 2H, 3′, 5′), 6.75 (d, 1H, 5), 4.84 (s, 1H, d), 4.62 (s, 1H, e), 3.95 (t, 2H, 7′), 3.80 (m, 1H, b), 3.76 (m, 2H, a, a′), 3.44 (m, 2H, c, c′), 2.08 (s, 3H, 7), 1.83 (m, 2H, 8′), 1.50 (m, 2H, 9′), and 0.95 (t, 3H, 10′); ^{13}C-NMR (ppm, 125 MHz, DMSO-d_6): δ= 190.2 (11), 162.4 (4′), 157.9 (4), 144.6 (β), 132.9 (1′), 131.4 (2, 2′, 6′), 129.4 (1), 128.2 (6), 127.1 (3), 122.6 (α), 114.4 (5, 3′, 5′), 70.8 (8, 9, 7′), 64.2 (10), 30.9 (8′), 16.4 (7, 9′), and 13.5 (10′). Elemental analysis for $C_{23}H_{28}O_5$: C, 71.85%; H, 7.34%; and O, 20.81%. Found: C, 71.77%; H, 7.42%; and O, 20.89%.

3-(4-(2,3-Dihydroxypropoxy)-3-methylphenyl)-1-(4-phenoxyphenyl)prop-2-en-1-one (A13):

Off white powder 0.218 g (54 % yield) (m.p.: 148-150 ˚C). R_f = 0.54; IR ν_{max} (cm^{-1}): 3282 (OH), 1650 (C=O); ^{1}H-NMR (ppm, 500 MHz,

DMSO-d_6): δ= 7.94 (d, 3H, 2′, 6′, β), 7.47 (m, 3H, 2, 6, α), 7.25 (t, 2H, 9′, 11′), 7.12 (t, 1H, 10′), 7.02 (d, 4H, 3′, 5′, 8′, 12′), 6.74 (d, 1H, 5), 4.85 (s, 1H, d), 4.62 (s, 1H, e), 3.81 (m, 1H, b), 3.73 (m, 2H, a, a′), 3.42 (m, 2H, c, c′), and 2.07 (s, 3H, 7); ^{13}C-NMR (ppm, 125 MHz, DMSO-d_6): δ= 189.3 (11), 157.7 (4, 7′), 149.7 (4′), 144.8 (β), 132.9 (1′), 131.9 (2, 2′, 6′), 129.8 (1, 9′, 11′), 128.5 (6), 127.4 (3), 124.4 (10′), 121.9 (α), 120.2 (3′, 5′), 118.6 (8′, 12′), 113.5 (5), 71.2 (8, 9), 63.6 (10), and 16.1 (7). Elemental analysis for $C_{25}H_{24}O_5$: C, 74.24%; H, 5.98%; and O, 19.78%. Found: C, 74.38%; H, 5.90%; and O, 19.84%.

1-([1, 1'-Biphenyl]-4-yl)-3-(4-(2,3-dihydroxypropoxy)-3-methylphenyl)prop-2-en-1-one (A14):

Pink powder 0.194 g (50 % yield) (m.p.: 190-192 ˚C). R_f = 0.62; IR ν_{max} (cm^{-1}): 3282 (OH), 1650 (C=O); ^{1}H-NMR (ppm, 500 MHz, DMSO-d_6): δ= 7.99 (d, 3H, 2′, 6′, β), 7.69 (d, 2H, 3′, 5′), 7.57 (d, 2H, 8′, 2′), 7.45 (m, 5H, 2, 6, α, 9′, 11′), 7.37 (t, 1H, 10′), 6.72 (d, 1H, 5), 4.80 (s, 1H, d), 4.60 (s, 1H, e), 3.85 (m, 1H, b), 3.74 (m, 2H, a, a′), 3.45 (m, 2H, c, c′), and 2.07 (s, 3H, 7); ^{13}C-NMR (ppm, 125 MHz, DMSO-d_6): δ= 190.4 (11), 158.1 (4), 144.5 (β, 4′), 140.2 (7′), 136.2 (1′), 131.6 (2), 129.8 (1, 2′, 6′, 9′, 11′), 128.4 (6), 127.6 (3, 3′, 5′, 8′, 10′, 12′), 121.8 (α), 113.5 (5), 70.7 (8, 9), 64.6 (10), and 16.2 (7). Elemental analysis for $C_{25}H_{24}O_4$: C, 77.30%; H, 6.23%; and O, 16.47%. Found: C, 77.38%; H, 6.27%; and O, 16.43%.

3-(4-(2,3-Dihydroxypropoxy)-3-methylphenyl)-1-(naphthalen-2-yl)prop-2-en-1-one (A15):

Yellow powder 0.192 g (53 % yield) (m.p.: 181-183 ˚C). R_f = 0.57; IR ν_{max} (cm^{-1}): 3282 (OH), 1644 (C=O); ^{1}H-NMR (ppm, 500 MHz, DMSO-d_6): δ= 8.45 (s, 1H, 6′), 7.95 (d, 5H, 2′, 3′, 7′, 10′, β), 7.58 (t, 1H, 9′), 7.45 (m, 4H, 2, 6, 8′, α), 6.77 (d, 1H, 5), 4.81 (s, 1H, d), 4.62 (s, 1H, e), 3.85 (m, 1H, b), 3.70 (m, 2H, a, a′), 3.41 (m, 2H, c, c′), and 2.10 (s, 3H, 7); ^{13}C-NMR (ppm, 125 MHz, DMSO-d_6): δ= 190.0 (11), 158.0 (4), 144.3 (β), 134.6 (1′, 4′, 5′), 131.5 (2), 129.4 (1, 6′, 10′), 128.4 (6, 3′, 7′), 127.4 (3, 2′, 9′), 126.1 (8′) 122.2 (α), 113.2 (5), 70.5 (8, 9), 64.1 (10), and 16.2 (7). Elemental analysis for $C_{23}H_{22}O_4$: C, 76.22%; H, 6.12%; and O, 17.66%. Found: C, 76.28%; H, 6.14%; and O, 17.62%.

3-(4-(2,3-Dihydroxypropoxy)-3-methylphenyl)-1-(6-methoxynaphthalen-2-yl)prop-2-en-1-one (A16):

Faint yellow powder 0.212 g (54 % yield) (m.p.: 184-186 ˚C). R_f = 0.55; IR ν_{max} (cm^{-1}): 3421 (OH), 1643 (C=O); ^{1}H-NMR (ppm, 500 MHz, DMSO-d_6): δ= 8.43 (s, 1H, 6′), 7.93 (d, 4H, 2′, 3′, 10′, β), 7.72 (d, 1H, 9′), 7.55 (d, 1H, 7′), 7.43 (m, 3H, 2, 6, α), 6.75 (d, 1H, 5), 4.84 (s, 1H, d), 4.64 (s, 1H, e), 3.83 (m, 4H, 11′, b), 3.72 (m, 2H, a, a′), 3.43 (m, 2H, c, c′), and 2.13 (s, 3H, 7); ^{13}C-NMR (ppm, 125 MHz, DMSO-d_6): δ= 189.6 (11), 157.5 (4, 8′), 144.6 (β), 135.2 (1′, 4′), 131.5 (2), 129.6 (1, 6′, 10′), 128.4 (6, 2′, 5′), 127.4 (3), 126.0 (3′) 122.2 (α), 113.6 (5, 9′), 109.8 (7′) 71.2 (8, 9), 63.9 (10), 55.4 (11′), and 15.9 (7). Elemental analysis for $C_{24}H_{24}O_5$: C, 73.45%; H, 6.16%; and O, 20.38%. Found: C, 73.53%; H, 6.20%; and O, 20.40%.

Biological testing

Antitumor evaluation

An MTT (3-(4,5-dimethyl-2-thiazolyl)-2,5-diphenyl-2Htetrazolium bromide) test, a tetrazolium salt, was used to measure antitumor activity, as previously described. [44,45] to get IC_{50} of (A7-A16) and adriamycin (positive control), as shown in table 1.

Antioxidant Activity

An 1, 1-Diphenyl-2-picryl Hydrazyl (DPPH) Assay was used to investigate antioxidant capacity as previously described [46-48]. The

IC_{50} value indicates the concentration of the sample needed to quench 50% of the DPPH free radicals, as presented in Table 2.

Method of Molecular Docking

The AutoDock Vina algorithm was used to dock the tested compounds against *Aquifex aeolicus* histone deacetylase homolog active site, where this homolog contains 375 residues that are identical to human HDAC1 (35.2%). The ligand that is co-crystallized inside the protein crystal (PDB code: 1C3S) obtained from the RCSB PDB generated the binding sites. The targeted proteins were prepared by removing water molecules, adding missing amino acids, correcting unfilled valence atoms, and minimizing the protein peptide energy by applying CHARMM force fields. A selection was made of the protein's essential amino acids, and preparations were made for testing them. Chem-Bio create Ultra17.0 was used to create the 2 dimensional orientation of the derivatives that were put to the test, and then the resulting drawings were saved in SDF file format. Protonation was performed on the ligands that were put through the test, and energy was reduced using the MMFF94 with an RMSD of 0.1 kcal/mol. After the structures were reduced, they were saved for molecular docking. Docking algorithms were used to carry out the process of molecular docking. While the target pocket was kept stiff throughout the process, the ligands were permitted to be flexible. During the refining process, it was permitted for each molecule to develop a total of twenty distinct interaction postures with the protein. Recorded were the docking scores, denoted by the symbol ΔG and representing the affinity interaction energy between the best-fitting postures and the active site of histone deacetylase [49, 50]. Utilizing the Discovery Studio 2016 visualizer program allowed for the generation of 3D orientation.

Results and discussion

Neoplastic suppressive results

Table 1 presents the findings of studies showing that the chalcones produced had a good interesting anti-neoplastic effect on all the various cancer cell lines tested. **A2** was the most potent, which may be attributable to the trifluoromethyl group inserted into position 4' of **A2** as part of the skeletal formula.

The beneficial trifluoromethyl substitution's influence on the aromatic system has been the subject of several studies [51-53], which has been found to slow the progression of malignancies.

TABLE 1 The study's findings assessed chalcone derivatives' potential to prevent neoplastic growth

Derivative	IC_{50} (μM) ± SD (n=3)				
	HepG2	MCF-7	HeLa	Ovcar-3	A549
Adriamycin	0.20 ± 0.01	0.06 ± 0.002	0.076 ± 0.003	0.06 ± 0.002	0.30 ± 0.01
A1	0.81 ± 0.02	0.97 ± 0.04	1.6 ± 0.06	1.01 ± 0.06	0.81 ± 0.03
A2	0.61 ± 0.02	0.54 ± 0.02	0.91 ± 0.05	0.60 ± 0.03	0.22 ± 0.01
A3	0.56 ± 0.02	0.86 ± 0.03	1.34 ± 0.08	0.72 ± 0.04	0.52 ± 0.03
A4	0.91 ± 0.05	0.66 ± 0.02	1.31 ± 0.04	1.32 ± 0.04	0.52 ± 0.01
A5	0.52 ± 0.02	0.75 ± 0.02	1.42 ± 0.05	0.71 ± 0.04	0.62 ± 0.02
A6	0.42 ± 0.01	0.94 ± 0.03	1.51 ± 0.06	0.72 ± 0.04	0.72 ± 0.03
A7	0.81± 0.03	0.97± 0.03	1.53± 0.03	1.12± 0.03	0.80± 0.03

A8	0.81± 0.03	0.91± 0.03	1.56± 0.03	1.12± 0.03	0.81± 0.03
A9	0.90± 0.03	1.12± 0.03	1.59± 0.03	1.32± 0.03	0.82± 0.03
A10	0.91± 0.03	1.02± 0.03	1.60± 0.03	1.32± 0.03	0.90± 0.03
A11	0.91± 0.03	1.08± 0.03	1.31± 0.03	1.18± 0.03	0.91± 0.03
A12	0.94± 0.03	1.18± 0.03	1.53± 0.03	1.28± 0.03	1.01± 0.03
A13	1.09± 0.03	1.40± 0.03	1.61± 0.03	2.52± 0.03	1.25± 0.03
A14	1.19± 0.03	1.30± 0.03	1.61± 0.03	2.71± 0.03	1.30± 0.03
A15	0.93± 0.03	1.00± 0.03	1.61± 0.03	2.00± 0.03	1.11± 0.03
A16	0.91± 0.03	1.10± 0.03	1.64± 0.03	2.03± 0.03	1.20± 0.03

Antioxidant activity results

Ascorbic acid, a common vitamin C supplement, was found to have an IC_{50} of 23.27µg/mL.

Among the sixteen new compounds examined for antioxidant activity using the DPPH approach, the compound **A2** produced in the previous work remains the excellent radical scavenger with strong antioxidant activity.

In contrast, the IC_{50} values for **A1, A3-A16** show moderate to low antioxidant activity [54]. Table 2 lists the data on antioxidant activity.

TABLE 2 The antioxidant activity of the produced chalcone derivatives (IC_{50} in µg/mL)

Derivative	IC_{50} ± SD (n=3)
A1	88.51 ± 3.4
A2	45.79 ± 1.8
A3	65.54 ± 3.2
A4	73.73 ± 1.8
A5	78.14 ± 2.7
A6	57.49 ± 2.2
A7	75.27 ± 3.9
A8	82.14 ± 4.1
A9	91.61 ± 5.0
A10	78.72 ± 4.3
A11	79.53 ± 3.1
A12	75.64 ± 4.0
A13	82.64 ± 4.7
A14	110.84 ± 7.2
A15	106.66 ± 6.1
A16	95.64 ± 5.1
Ascorbic acid	23.27 ± 1.2

The outcomes of docking

The docking findings of the compounds, including the predicted values for their free binding energies ΔG (Docking Score) (kcal/mol), as well as the interactions that occur with important amino acid residues at the active site of homolog, are expressed in Table 3 and Figures (2-10). All compounds showed hydrogen and pi interactions at the active site of *Aquifex aeolicus* HDAC homolog, and most of them had bond dipole-ion interaction with Zinc ion (Zn^{+2}).

TABLE 3 (ΔG) kcal/mol of (A1-A16) and vorinostat (SAHA) against (*Aquifex aeolicus* HDAC homolog) target site (PDB ID: 1C3S)

Compound	RMSD value (Å)	ΔG (kcal/mol)	Interactions	
			Hydrogen Binding	π-interactions
Compound A1	1.50	-9.34	2	6
Compound A2	1.52	-9.54	2	8
Compound A3	1.01	-9.53	1	11
Compound A4	1.29	-9.45	1	6
Compound A5	1.35	-9.09	2	5
Compound A6	1.56	-9.79	3	5
Compound A7	1.51	-9.45	2	5
Compound A8	1.27	-9.76	2	5
Compound A9	1.46	-9.97	3	7
Compound A10	1.53	-10.10	1	6
Compound A11	1.69	-9.85	2	6
Compound A12	1.50	-9.44	1	9
Compound A13	1.28	-10.69	2	7
Compound A14	1.28	-10.25	2	9
Compound A15	1.27	-9.86	2	10
Compound A16	1.77	-9.82	-	6
SAHA	1.22	-10.33	3	1

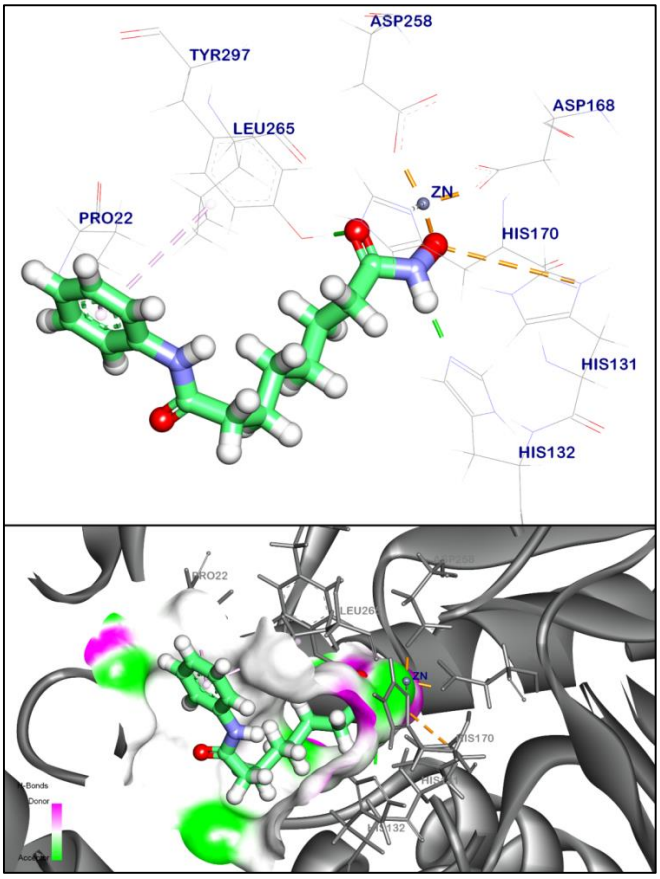

FIGURE 2 Mapping surface and 3d representation of the co-crystalized ligand (SAHA) docked in *Aquifex aeolicus* HDAC homolog

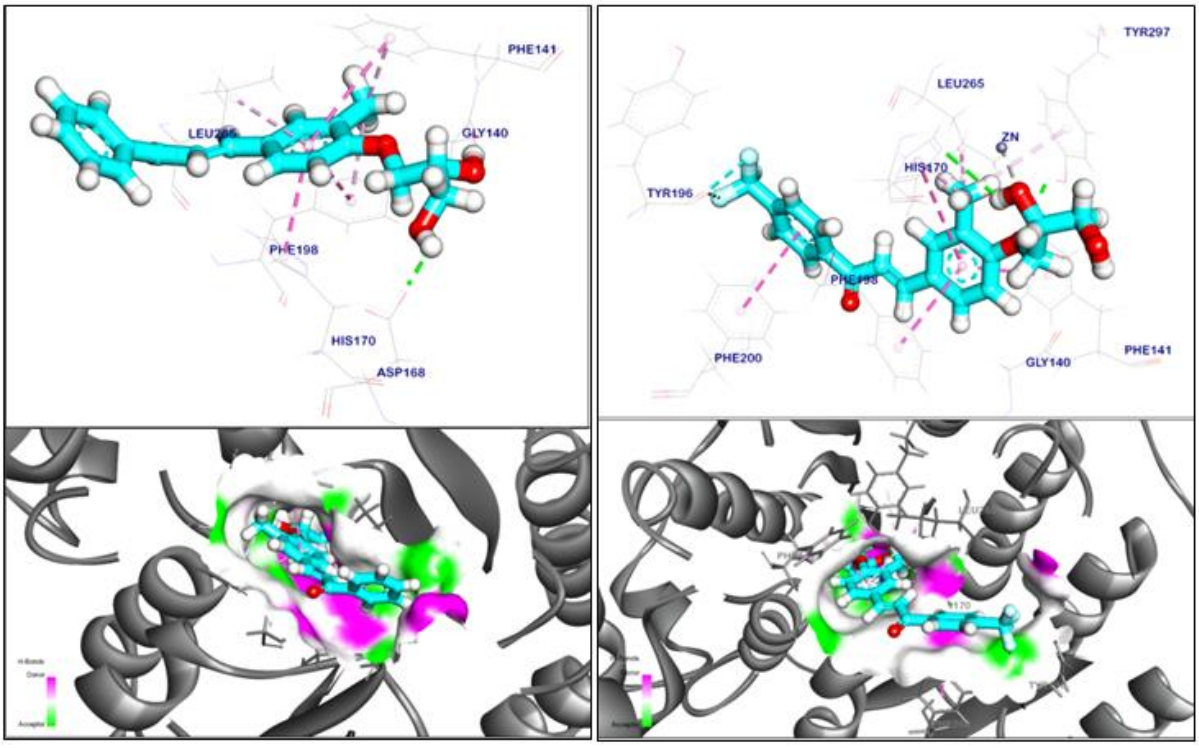

FIGURE 3 Mapping surface and 3d orientation of compound A1 (left), compound A2 (right) docked in *Aquifex aeolicus* HDAC homolog

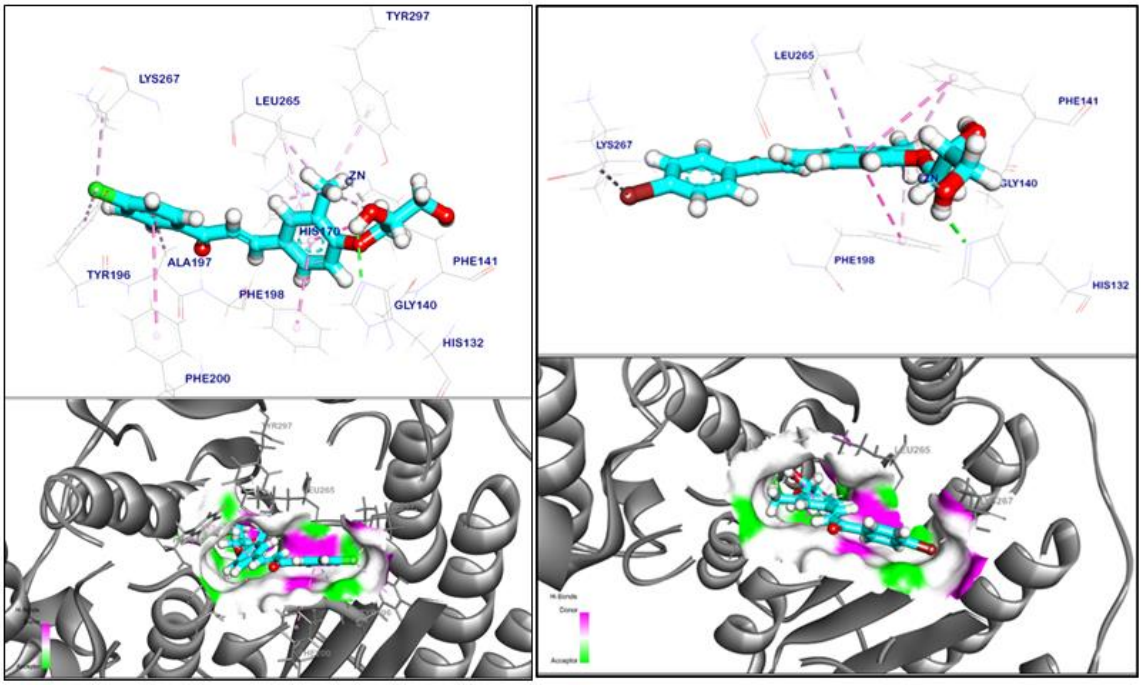

FIGURE 4 Mapping surface and 3d orientation of compound A3 (left), compound A4 (right) docked in *Aquifex aeolicus* HDAC homolog

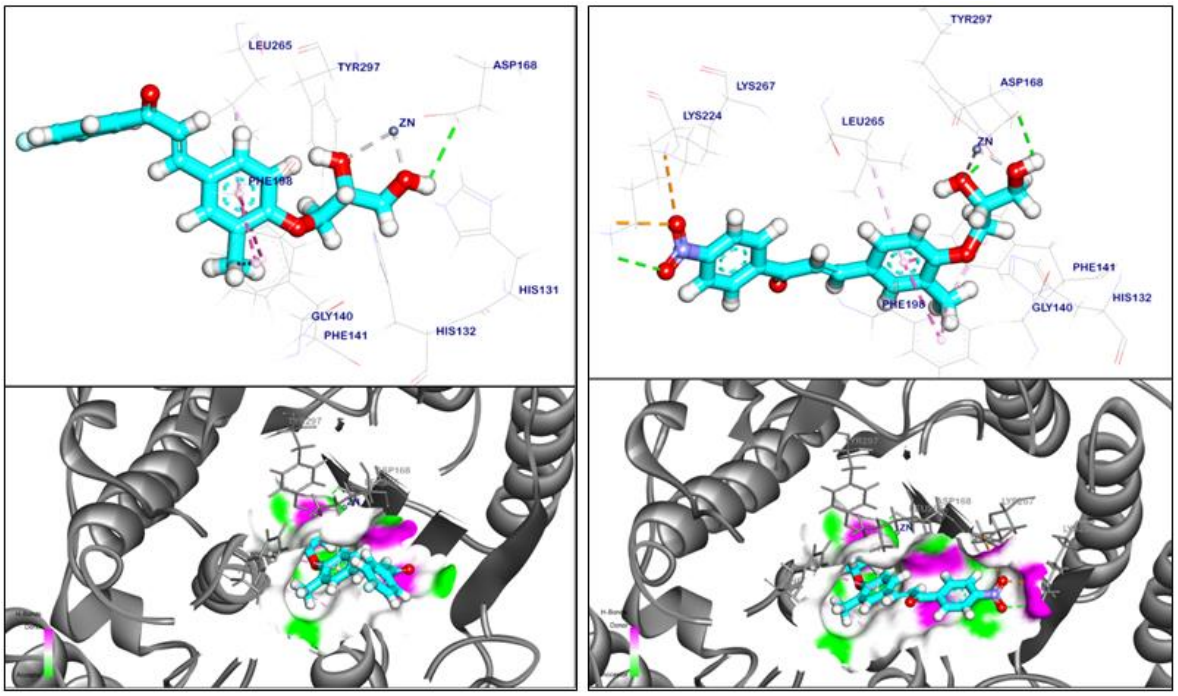

FIGURE 5 Mapping surface and 3d orientation of compound A5 (left), compound A6 (right) docked in *Aquifex aeolicus* HDAC homolog

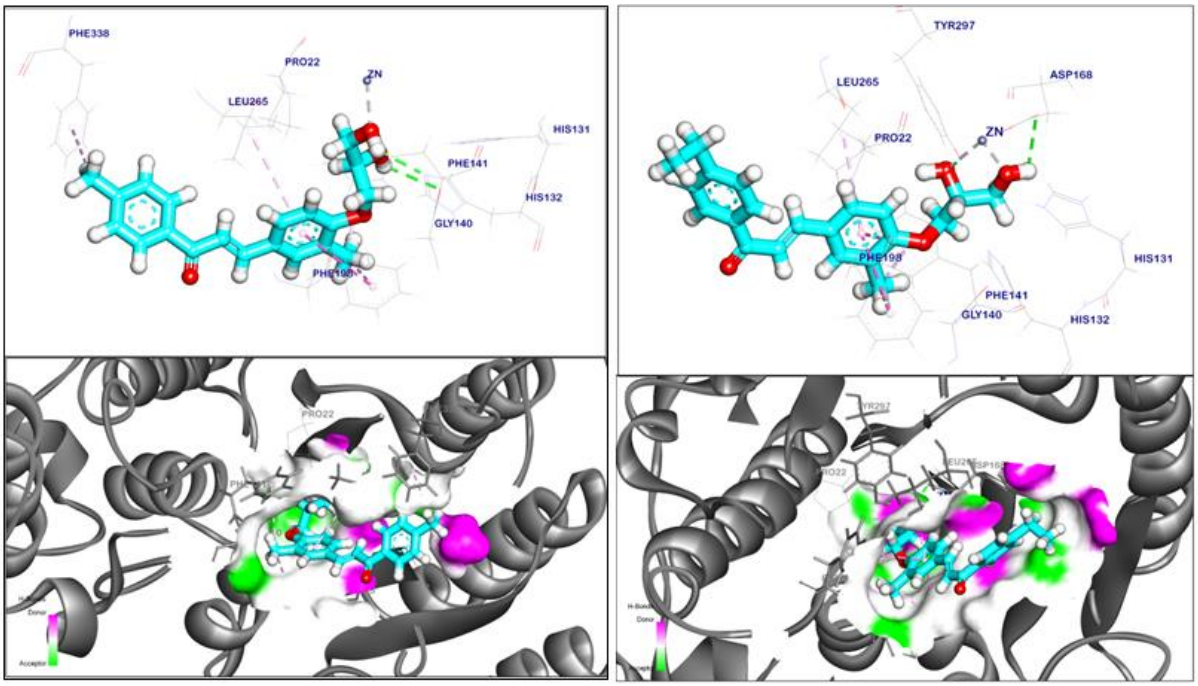

FIGURE 6 Mapping surface and 3d orientation of compound A7 (left), compound A8 (right) docked in *Aquifex aeolicus* HDAC homolog

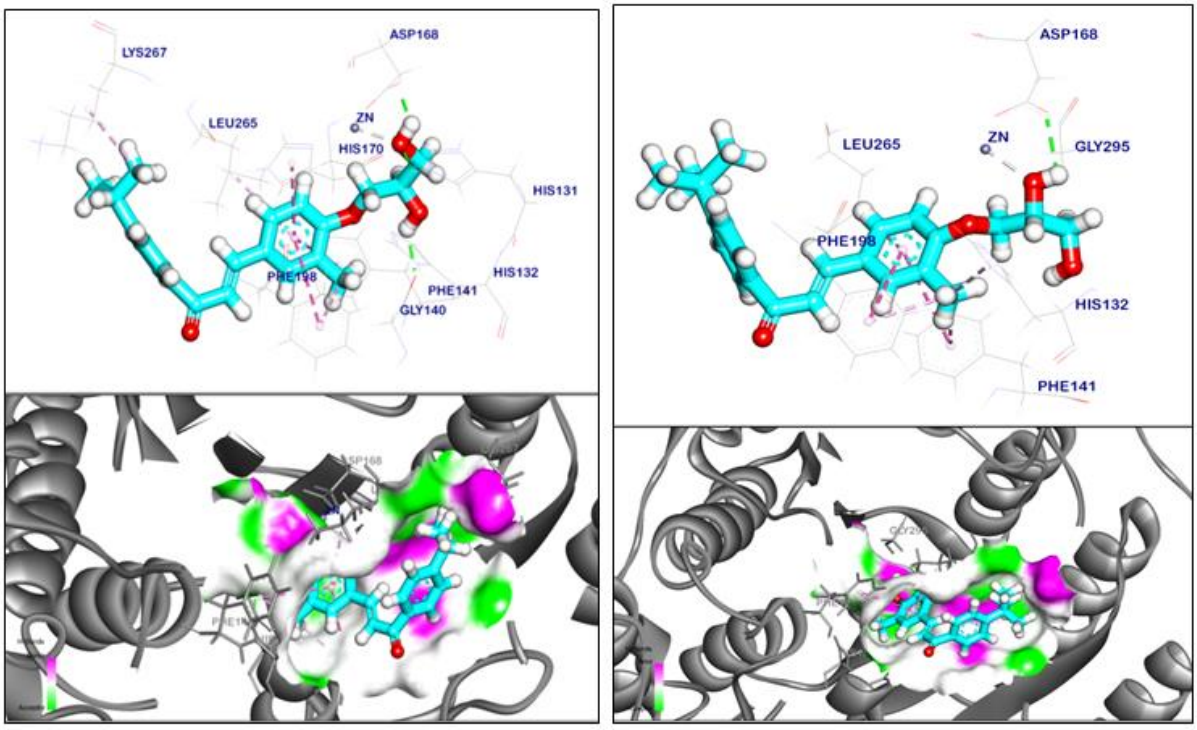

FIGURE 7 Mapping surface and 3d orientation of compound A9 (left), compound A10 (right) docked in *Aquifex aeolicus* HDAC homolog

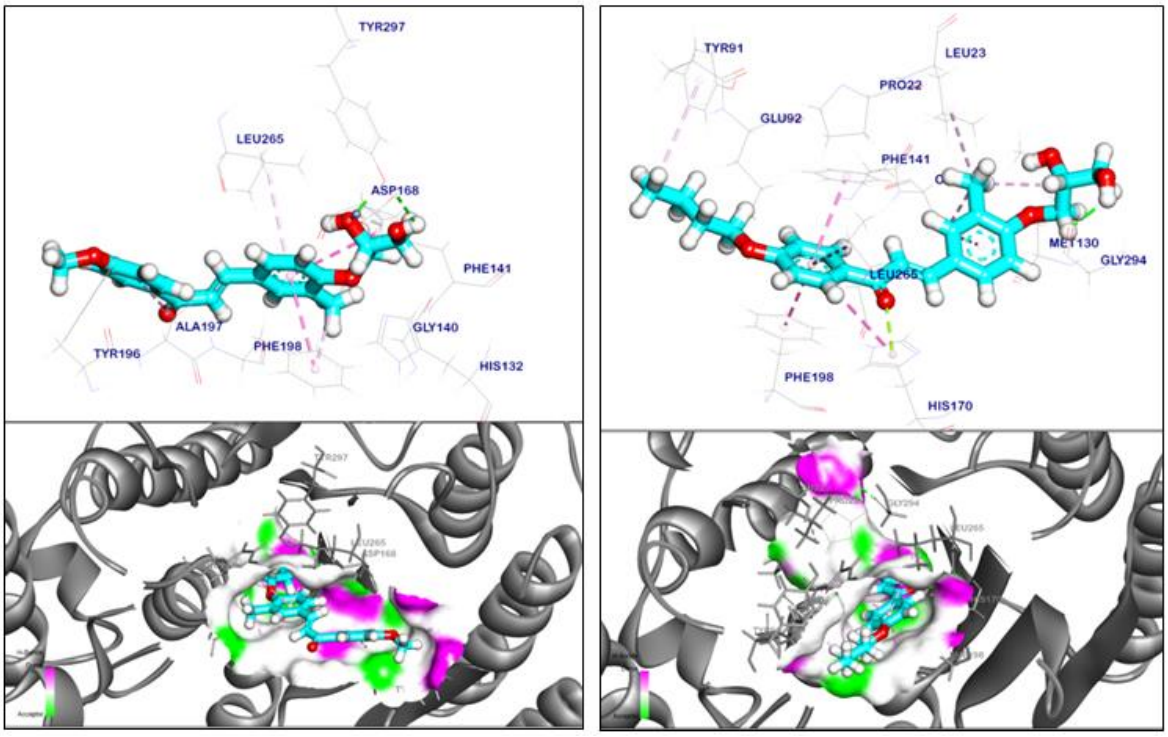

FIGURE 8 Mapping surface and 3d orientation of compound A11 (left), compound A12 (right) docked in *Aquifex aeolicus* HDAC homolog

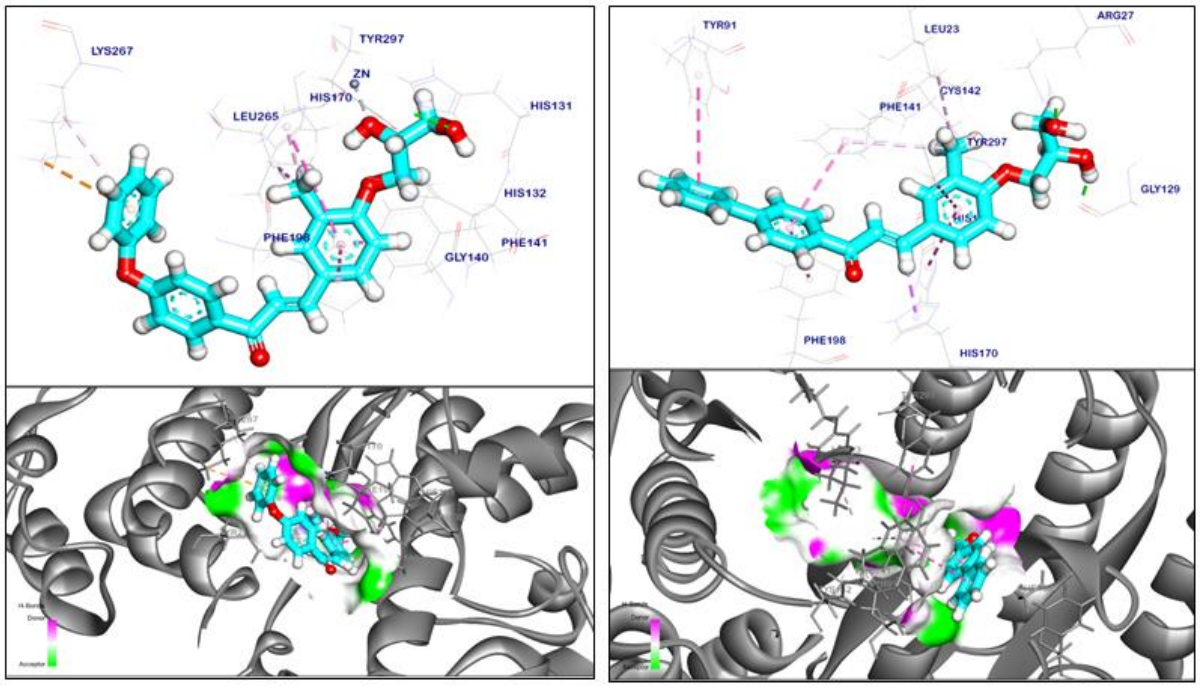

FIGURE 9 Mapping surface and 3d orientation of compound A13 (left), compound A14 (right) docked in *Aquifex aeolicus* HDAC homolog

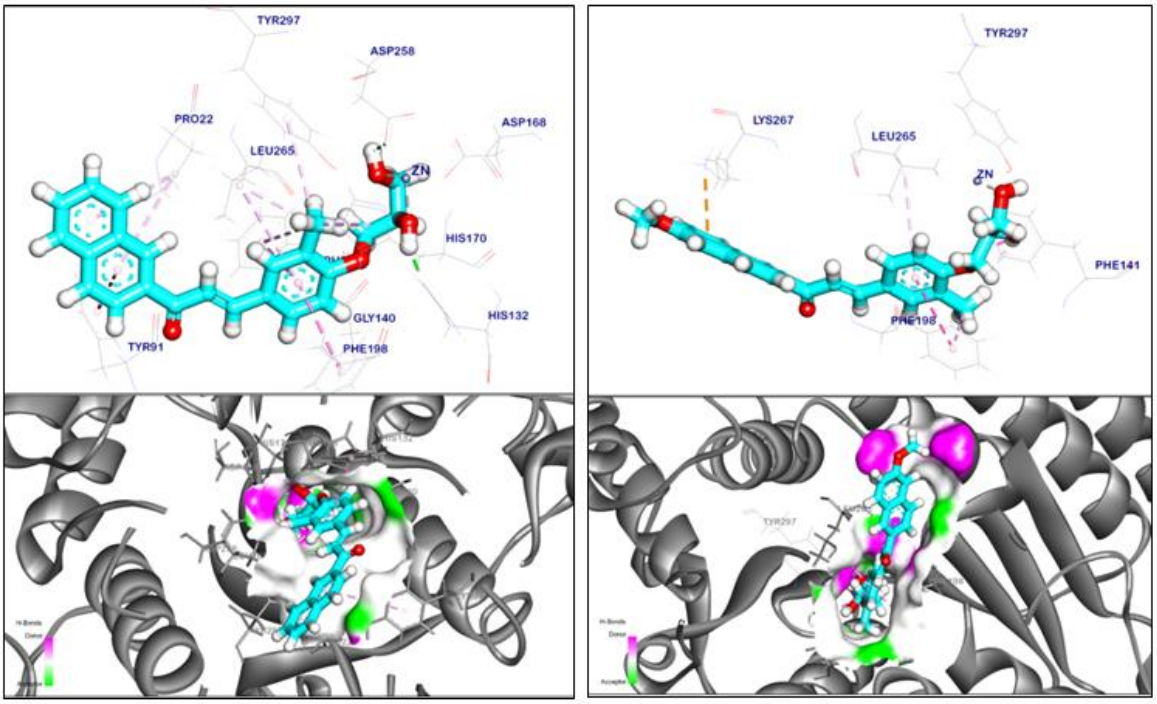

FIGURE 10 Mapping surface and 3d orientation of compound A15 (left), compound A16 (right) docked in *Aquifex aeolicus* HDAC homolog

Pharmacokinetic study (ADMET studies)

ADMET studies

Biovia Discovery Studio 2019 was used to analyze the results of the ADMET studies [55,56]. All ligands were shown to have high to very high permeability across the brain-blood barrier (BBB), with the exception of A6, which exhibited low permeability, and SAHA exhibited medium permeability. Except for SAHA, which showed excellent solubility, other ligands ranged from poorly soluble to very soluble.

In addition, the ligands demonstrated high rates of absorption and showed no signs of inhibiting cytochrome P450. Regarding their potential to cause damage to the liver, none of the ligands were considered hazardous.

Finally, it was determined that all ligands, with the exception of SAHA, had a probability of binding plasma protein (PPB) that was more than 90%. All ligands were shown to have favorable pharmacokinetic characteristics, justifying their selection for future study (Figure 11) and (Table 4).

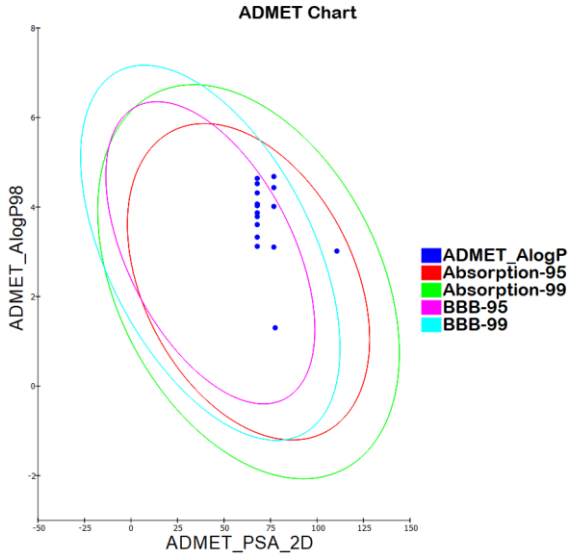

FIGURE 11 ADMET outcomes predicted for the synthesized chalcone derivatives

TABLE 4 ADMET predictions for the synthesized chalcones (A1-A16)

Compound	BBB level [a]	Solubility level [b]	Absorption level [c]	Hepatotoxicity	CYP2D6 prediction [d]	PPB prediction [e]
Compound A1	2	3	0	Negative	Negative	Positive
Compound A2	1	2	0	Negative	Negative	Positive
Compound A3	2	3	0	Negative	Negative	Positive
Compound A4	2	3	0	Negative	Negative	Positive
Compound A5	2	3	0	Negative	Negative	Positive
Compound A6	4	3	0	Negative	Negative	Positive
Compound A7	2	3	0	Negative	Negative	Positive
Compound A8	1	3	0	Negative	Negative	Positive
Compound A9	1	3	0	Negative	Negative	Positive
Compound A10	1	2	0	Negative	Negative	Positive
Compound A11	2	3	0	Negative	Negative	Positive
Compound A12	1	3	0	Negative	Negative	Positive
Compound A13	1	2	0	Negative	Negative	Positive
Compound A14	1	2	0	Negative	Negative	Positive
Compound A15	1	2	0	Negative	Negative	Positive
Compound A16	2	2	0	Negative	Negative	Positive
SAHA	3	4	0	Negative	Negative	Negative

[a]BBB level, blood brain barrier level, 4 = very low, 3 = low, 2 = medium, 1 = high, and 0 = very high.
[b]Solubility level, 4 = optimal, 3 = good, 2 = low, and 1 = very low.
[c]Absorption level, 3 = very poor, 2 = poor, 1 = moderate, and 0 = good.
[d]CYP2D6, cytochrome P2D6, Negative = non inhibitor and Positive = inhibitor.
[e]Predicted plasma protein binding. Positive means more than 90%, and Negative means less than 90%.The categorization of whether a molecule is strongly bound (bound to at least 90% of plasma proteins) using a cut-off Bayesian score of -2.209 as the determining factor.

Conclusion

The pharmacological relevance of chalcone scaffolds provides vast possibilities for the discovery of new drugs with unique mechanisms of action. In this study, a number of chalcone derivatives were produced, and their *in vitro* anticancer and antioxidant characteristics were evaluated (A1-A16) with a 3-propoxy-1, 2-diol arm as (ZBG). While the results indicated that all compounds could have some anti-cancer properties, compound

A2 proved to be the most effective. Docking and cytotoxicity studies yielded the following results: compound **A2** is a good *lead molecule for novel HDACIs* with alkyl 1, 2-diol as (ZBG).

Acknowledgements

The Pharmacy Faculty in the University of Baghdad generously provided the necessary facilities, which greatly improved the overall quality of the study.

Conflict of Interest

The authors certify that they do not have any financial or other conflicts of interest for this article.

Orcid:

Ahmed Abdulwahid Sadon:
https://orcid.org/0009-0005-2053-379X
Shihab Hattab Mutlag:
https://orcid.org/0000-0002-5361-8221
Raheem Jameel Mohaisen:
https://orcid.org/0000-0002-5651-2924

References

[1] G. Wang, W. Liu, Z. Gong, Y. Huang, Y. Li, Z. Peng, Design, synthesis, biological evaluation and molecular docking studies of new chalcone derivatives containing diaryl ether moiety as potential anticancer agents and tubulin polymerization inhibitors, *Bioorg. Chem.*, **2020**, *95*, 103565. [Crossref], [Google Scholar], [Publisher]

[2] M.M. Al-Sanea, A. Hamdi, A.A.B. Mohamed, H.W. El-Shafey, M. Moustafa, A.A. Elgazar, W.M. Eldehna, H.U. Rahman, D.G.T. Parambi, R.M. Elbargisy, S. Selim, S.N.A. Bukhari, O.M. Hendawy, S.S. Tawfikb, New benzothiazole hybrids as potential VEGFR-2 inhibitors: design, synthesis, anticancer evaluation, and *in silico* study, *J. Enzyme. Inhib. Med. Chem.*, **2023**, *38,* 2166036. [Crossref], [Google Scholar], [Publisher]

[3] S.A. Mir, G.C. Dash, R.K. Meher, P.P. Mohanta, K.S. Chopdar, P.K. Mohapatra, I. Baitharu, A.K. Behera, M.K. Raval, B. Nayak, In silico and in vitro evaluations of fluorophoric thiazolo-[2,3-b]quinazolinones as anti-cancer agents targeting EGFR-TKD, *Appl. Biochem. Biotechnol.*, **2022,** *194*, 4292-4318. [Crossref], [Google Scholar], [Publisher]

[4] A. Phaniendra, D.B. Jestadi, L. Periyasamy, Free radicals: properties, sources, targets, and their implication in various diseases, *Indian J. Clin. Biochem.,* **2015**, *30,* 11-26. [Crossref], [Google Scholar], [Publisher]

[5] R.A. Zinovkin, K.G. Lyamzaev, B.V. Chernyak, Current perspectives of mitochondria-targeted antioxidants in cancer prevention and treatment, *Front. Cell. Dev. Biol.*, **2023,** *11,* 1048177. [Crossref], [Google Scholar], [Publisher]

[6] K. Cen, Z. Wu, Y. Mai, Y. Dai, K. Hong, Y. Guo, Identification of a novel reactive oxygen species (ROS)-related genes model combined with RT-qPCR experiments for prognosis and immunotherapy in gastric cancer, *Front Genet.*, **2023**, *14,* 1074900. [Crossref], [Google Scholar], [Publisher]

[7] N. Mut-Salud, P.J. Álvarez, J.M. Garrido, E. Carrasco, A. Aránega, F. Rodríguez-Serrano, Antioxidant intake and antitumor therapy: toward nutritional recommendations for optimal results, *Oxid. Med. Cell Longev.*, **2016**, *2016,* 6719534. [Crossref], [Google Scholar], [Publisher]

[8] M. Apotrosoaei, I. Vasincu, S. Constantin, F. Buron, S. Routier, L. Profire, Synthesis, characterization and antioxidant activity of some new thiazolidin-4-one derivatives, *Rev. Med. Chir. Soc. Med. Nat. Iasi.*, **2014**, *118,* 213-218. [Pdf], [Google Scholar], [Publisher]

[9] C. Danciu, L. Vlaia, F. Fetea, M. Hancianu, D.E. Coricovac, S.A. Ciurlea, C.M. Şoica, I. Marincu, V. Vlaia, C.A. Dehelean, C. Trandafirescu, evaluation of phenolic profile, antioxidant and anticancer potential of two main representants of Zingiberaceae family against B164A5 murine melanoma cells, *Biol.*

Res., **2015,** *48*, 1. [Crossref], [Google Scholar], [Publisher]

[10] M. Demurtas, A. Baldisserotto, I. Lampronti, D. Moi, G. Balboni, S. Pacifico, S. Vertuani, S. Manfredini, V. Onnis, Indole derivatives as multifunctional drugs: Synthesis and evaluation of antioxidant, photoprotective and antiproliferative activity of indole hydrazones, *Bioorg. Chem*., **2019**, *85*, 568-576. [Crossref], [Google Scholar], [Publisher]

[11] Q. Li, J. Chen, S. Luo, J. Xu, Q. Huang, T. Liu, Synthesis and assessment of the antioxidant and antitumor properties of asymmetric curcumin analogues, *Eur. J. Med. Chem*., **2015**, *93,* 461-469. [Crossref], [Google Scholar], [Publisher]

[12] A. Mishra, P.K. Prabha, R. Singla, G. Kaur, A.R. Sharma, R. Joshi, B. Suroy, B. Medhi, Epigenetic interface of autism spectrum disorders (ASDs): implications of chromosome 15q11–q13 segment, *ACS Chem. Neurosci.*, **2022**, *13*, 1684–1696. [Crossref], [Google Scholar], [Publisher]

[13] T. Zykova, M. Maltseva, F. Goncharov, L. Boldyreva, G. Pokholkova, T. Kolesnikova, I. Zhimulev, The organization of pericentromeric heterochromatin in polytene chromosome 3 of the *Drosophilamelanogaster* line with the *Rif*^{1}*; SuUR*^{ES} *Su(var)3-9*^{06} mutations suppressing underreplication, *Cells,* **2021**, *10*, 2809. [Crossref], [Google Scholar], [Publisher]

[14] Z. Hu, F. Wei, Y. Su, Y. Wang, Y. Shen, Y. Fang, J. Ding, Y. Chen, Histone deacetylase inhibitors promote breast cancer metastasis by elevating NEDD9 expression, *Sig. Transduct. Target. Ther.*, **2023**, *8*, 11. [Crossref], [Google Scholar], [Publisher]

[15] B. Carmona, H.S. Marinho, C.L. Matos, S. Nolasco, H. Soares, Tubulin post-translational modifications: the elusive roles of acetylation, *Biology*, **2023**, *12*, 561. [Crossref], [Google Scholar], [Publisher]

[16] M. Sandonà, G. Cavioli, A. Renzini, A. Cedola, G. Gigli, D. Coletti, T.A. McKinsey, V. Moresi, V. Saccone, Histone deacetylases: molecular mechanisms and therapeutic implications for muscular dystrophies, *Int. J. Mol. Sci*., **2023**, *24*, 4306. [Crossref], [Google Scholar], [Publisher]

[17] L. Li, S. Hao, M. Gao, J. Liu, X. Xu, J. Huang, G. Cheng, H. Yang, $HDAC_3$ Inhibition promotes antitumor immunity by enhancing CXCL10-mediated chemotaxis and recruiting of immune cells, *Cancer. Immunol. Res*., **2023**, *11*, 657-673. [Crossref], [Google Scholar], [Publisher]

[18] M.J. Ramaiah, A.D. Tangutur, R.R. Manyam, Epigenetic modulation and understanding of HDAC inhibitors in cancer therapy, *Life Sci*., **2021**, *277*, 119504. [Crossref], [Google Scholar], [Publisher]

[19] D.H. Al-Amily, M.H. Mohammed, Design, synthesis and cytotoxicity study of primary amides as histone deacetylase inhibitors, *Iraqi J. Pharm. Sci.,* **2019**, *28*, 151-158. [Crossref], [Google Scholar], [Publisher]

[20] D.H. Al-Amily, M.H. Mohammed, Design, synthesis, and docking study of acyl thiourea derivatives as possible histone deacetylase inhibitors with a novel zinc binding group, *Sci. Pharm.*, **2019**, *87*, 28. [Crossref], [Google Scholar], [Publisher]

[21] O.M. Sagheer, M.H. Mohammed, Z.O. Ibraheem, J.S. Wadi, M.F. Tawfeeq, Synthesis of gamma biguanides butyric acid analogues as HDAC inhibitors and studying their cytotoxic activity, *Mater. Today: Proc*., **2021**, *47*, 5983-5991. [Crossref], [Google Scholar], [Publisher]

[22] O.M. Sagheer, M.H. Mohammed, J. Wadi, Studying the cytotoxic activity of newly designed and synthesized HDAC inhibitors derivatives of pentanoyl anilide-5-biguanide, *Macromol. Symp*., **2022**, *401*, 2100346. [Crossref], [Google Scholar], [Publisher]

[23] W. Dan, J. Dai, Recent developments of chalcones as potential antibacterial agents in medicinal chemistry, *Eur. J. Med. Chem*., **2020**, *187*, 111980. [Crossref], [Google Scholar], [Publisher]

[24] S. Sinha, B. Medhi, B.D. Radotra, D.I. Batovska, N. Markova, A. Bhalla, R. Sehgal, Antimalarial and immunomodulatory potential of chalcone derivatives in experimental model of malaria, *BMC Complement. Med. Ther.*, **2022**, *22*, 330. [Crossref], [Google Scholar], [Publisher]
[25] Q. Zhou, X. Tang, S. Chen, W. Zhan, D. Hu, R. Zhou, N. Sun, Y. Wu, W. Xue, Design, synthesis, and antifungal activity of novel chalcone derivatives containing a piperazine fragment, *J. Agric. Food Chem.,* **2022**, *70*, 1029-1036. [Crossref], [Google Scholar], [Publisher]
[26] P. Thapa, S.P. Upadhyay, W.Z. Suo, V. Singh, P. Gurung, E.S. Lee, R. Sharma, M. Sharma, Chalcone and its analogs: Therapeutic and diagnostic applications in Alzheimer's disease, *Bioorg. Chem.* **2021**, *108*, 104681. [Crossref], [Google Scholar], [Publisher]
[27] N. Ohkura, K. Ohnishi, M. Taniguchi, A. Nakayama, Y. Usuba, M. Fujita, A. Fujii, K. Ishibashi, K. Baba, G. Atsumi, Anti-platelet effects of chalcones from *Angelica keiskei* Koidzumi (Ashitaba) *in vivo*, *Pharmazie*. **2016**, *71*, 651-654. [Crossref], [Google Scholar], [Publisher]
[28] S.A. Lahsasni, F.H. Al Korbi, N.A. Aljaber, Synthesis, characterization and evaluation of antioxidant activities of some novel chalcones analogues, *Chem. Cent. J.,* **2014**, *8*, 32. [Crossref], [Google Scholar], [Publisher]
[29] H. Rashid, Y. Xu, N. Ahmad, Y. Muhammad, L. Wang, Promising anti-inflammatory effects of chalcones via inhibition of cyclooxygenase, prostaglandin E_2, inducible NO synthase and nuclear factor κb activities, *Bioo. Chem.,* **2019**, *87*, 335-365. [Crossref], [Google Scholar], [Publisher]
[30] A. Pasha, S. Mondal, N. Panigrahi, Synthesis of novel aryl (4-aryl-1H-pyrrol-3-yl) (thiophen-2-yl) methanone derivatives: molecular modelling, in silico ADMET, anti-inflammatory and anti-ulcer activities, *Antiinflamm, Antiallergy Agents Med. Chem.,* **2021**, 20, 182-195. [Crossref], [Google Scholar], [Publisher]
[31] T. Constantinescu, C.N. Lungu, Anticancer activity of natural and synthetic chalcones, *Int, J. Mol. Sci*., **2021**, *22*, 11306. [Crossref], [Google Scholar], [Publisher]
[32] Y. Ouyang, J. Li, X. Chen, X. Fu, S. Sun, Q. Wu, Chalcone derivatives: role in anticancer therapy, *Biomolecules*, **2021**, *11*, 894. [Crossref], [Google Scholar], [Publisher]
[33] M. Das, K. Manna, Chalcone scaffold in anticancer armamentarium: a molecular insight, *J. Toxicol.,* **2016**, *2016*, 7651047. [Crossref], [Google Scholar], [Publisher]
[34] A.A. WalyEldeen, S. Sabet, H.M. El-Shorbagy, I.A. Abdelhamid, S.A. Ibrahim, Chalcones: Promising therapeutic agents targeting key players and signaling pathways regulating the hallmarks of cancer, *Chem. Biol. Interact*., **2023**, *369*, 110297. [Crossref], [Google Scholar], [Publisher]
[35] L. Goracci, N. Deschamps, G.M. Randazzo, C. Petit, C.D.S. Passos, P.A. Carrupt, C. Simões-Pires, A. Nurisso, A rational approach for the identification of non-hydroxamate HDAC6-selective inhibitors, *Sci. Rep*., **2016**, *6*, 29086. [Crossref], [Google Scholar], [Publisher]
[36] K.C. Hsu, C.Y. Liu, T.E. Lin, J.H. Hsieh, T.Y. Sung, H.J. Tseng, J.M. Yang, W.J. Huang, Novel class iIa-selective histone deacetylase inhibitors discovered using an in silico virtual screening approach, *Sci. Rep*., **2017**, *7*, 3228. [Crossref], [Google Scholar], [Publisher]
[37] B. Orlikova, M. Schnekenburger, M. Zloh, F. Golais, M. Diederich, D. Tasdemir, Natural chalcones as dual inhibitors of HDACs and NF-Kb, *Oncol. Rep*., **2012**, *28*, 797-805. [Crossref], [Google Scholar], [Publisher]
[38] M.F.A. Mohamed, M.S.A. Shaykoon, M.H. Abdelrahman, B.E.M. Elsadek, A.S. Aboraia, G.E.A.A. Abuo-Rahma, Design, synthesis, docking studies and biological evaluation of novel chalcone derivatives as potential histone deacetylase inhibitors, *Bioorg. Chem*.,

2017, *72*, 32-41. [Crossref], [Google Scholar], [Publisher]
[39] A.A. Sadon, S.H. Mutlag, R.J. Mohaisen, Synthesis and preliminary biological assessment of novel chalcone derivatives derived from Duff's formylated mephenesin, *Eurasian Chem. Commun.*, **2023**, *5*, 701-711. [Crossref], [Pdf], [Publisher]
[40] F.W. Askar, Y.A. Aldheif, N.A. Jinzeel, O.A. Nief, Synthesis and biological activity evaluation of new sulfonamid derivatives, *Iraqi J. Sci.*, **2017**, *58*, 2012–2021. [Pdf], [Google Scholar], [Publisher]
[41] J.H. Tomma, D.F. Hussein, N.M. Jamel, Synthesis and characterization of some new quinoline-2-one, schiff bases, pyrazole and pyrazoline compounds derived from hydrazide containing isoxazoline or pyrimidine cycles, *Iraqi J. Sci.*, **2016**, *57*, 1316–1332. [Google Scholar], [Publisher]
[42] T.W. Jihad, A.S. Alkazzaz, Synthesis of a series of α, β-unsaturated ketoximes and their corresponding acetate esters, *Iraqi J. Sci.*, **2022**, *63*, 4142–4151. [Crossref], [Google Scholar], [Publisher]
[43] T.S. Ghali, J.H. Tomma, Synthesis and characterization of indazol-3-one and thioxo pyrimidines derivatives from mono and twin chalcones, *Iraqi J. Sci.*, **2017**, *58*, 2265-2277. [Crossref], [Google Scholar], [Publisher]
[44] M. Ghasemi, T. Turnbull, S. Sebastian, I. Kempson, The MTT assay: utility, limitations, pitfalls, and interpretation in bulk and single-cell analysis, *Int. J. Mol. Sci.*, **2021**, *22*, 12827. [Crossref], [Google Scholar], [Publisher]
[45] S.A. Abdullah, A.M. Al-Shammari, S.A. Lateef, Attenuated measles vaccine strain have potent oncolytic activity against Iraqi patient derived breast cancer cell line, *Saudi. J. Biol. Sci.*, **2020**, *27*, 865-872. [Crossref], [Google Scholar], [Publisher]
[46] L. Zheng, L. Lin, G. Su, Q. Zhao, M. Zhao, Pitfalls of using 1,1-diphenyl-2-picrylhydrazyl (DPPH) assay to assess the radical scavenging activity of peptides: Its susceptibility to interference and low reactivity towards peptides, *Food Res. Int.*, **2015**, *76*, 359-365. [Crossref], [Google Scholar], [Publisher]
[47] A. Tai, K. Fukunaga, A. Ohno, H. Ito, Antioxidative properties of ascorbigen in using multiple antioxidant assays, *Biosci. Biotechnol. Biochem.*, **2014**, *78*, 1723-1730. [Crossref], [Google Scholar], [Publisher]
[48] S. Baliyan, R. Mukherjee, A. Priyadarshini, A. Vibhuti, A. Gupta, R.P. Pandey, C.M. Chang, Determination of antioxidants by DPPH radical scavenging activity and quantitative phytochemical analysis of *Ficus religiosa*, *Molecules.*, **2022**, *27*, 1326. [Crossref], [Google Scholar], [Publisher]
[49] S. Tang, R. Chen, M. Lin, Q. Lin, Y. Zhu, J. Ding, H. Hu, M. Ling, J. Wu, Accelerating AutoDock Vina with GPUs, *Molecules*, **2022**, *27*, 3041. [Crossref], [Google Scholar], [Publisher]
[50] T.F. Vieira, S.F. Sousa, Comparing auto dock and Vina in ligand/decoy Discrimination for virtual screening, *Appl. Sci.*, **2019**, *9*, 4538. [Crossref], [Google Scholar], [Publisher]
[51] A.S. Sawant, S.S. Kamble, P.M. Pisal, S.S. Sawant, S.V. Hese, K.T. Bagul, R.V. Pinjari, V.T. Kamble, R.J. Meshram, R.N. Gacche, Synthesis and evaluation of N-(4-(substituted)-3-(trifluoromethyl) phenyl) isobutyramides and their N-ethyl analogous as anticancer, anti-angiogenic & antioxidant agents: *In vitro* and *in silico* analysis, *Comput. Biol. Chem.*, **2021**, *92*, 107484. [Crossref], [Google Scholar], [Publisher]
[52] S.M. Kwon, Y.Y. Jung, C.J. Hwang, M.H. Park, N.Y. Yoon, T.M. Kim, J.M. Yu, D.H. Kim, D.W. Seo, H.S. Youn, H.O. Seo, I.S. Chung, S.B. Han, B.Y. Hwang, H.S. Yoo, J.K. Jung, H. Lee, J.T. Hong, Anti-cancer effect of N-(3,5-bis(trifluoromethyl)phenyl)-5-chloro-2,3-dihydronaphtho[1,2-b]furan-2-carboxamide, a novel synthetic compound, *Mol. Carcinog.*, **2016**, *55*, 659-670. [Crossref], [Google Scholar], [Publisher]
[53] Y. Saito, A. Mizokami, K. Izumi, R. Naito, M. Goto, K. Nakagawa-Goto, α-Trifluoromethyl chalcones as potent

anticancer agents for androgen receptor-independent prostate cancer, *Molecules,* **2021**, *26*, 2812. [Crossref], [Google Scholar], [Publisher]

[54] A. Itam, M.S. Wati, V. Agustin, N. Sabri, R. A. Jumanah, M. Efdi, Comparative study of phytochemical, antioxidant, and cytotoxic activities and phenolic content of *Syzygium aqueum* (Burm. f. Alston f.) extracts growing in West Sumatera Indonesia, *Sci. World J.,* **2021**, *2021*, 5537597. [Crossref], [Google Scholar], [Publisher]

[55] N. Flores-Holguín, J. Frau, D. Glossman-Mitnik, Computational pharmacokinetics report, ADMET study and conceptual DFT-based estimation of the chemical reactivity properties of marine cyclopeptides, *ChemistryOpen*, **2021**, *10*, 1142-1149. [Crossref], [Google Scholar], [Publisher]

[56] I. Ahmad, A.E. Kuznetsov, A.S. Pirzada, K.F. Alsharif, M. Daglia, H. Khan, Computational pharmacology and computational chemistry of 4-hydroxyisoleucine: physicochemical, pharmacokinetic, and DFT-based approaches, *Front. Chem*., **2023**, *11*, 1145974. [Crossref], [Google Scholar], [Publisher]

How to cite this article: Ahmed Abdulwahid Sadon*, Shihab Hattab Mutlag, Raheem Jameel Mohaisen. In silico study of chalcones having novel zinc binding group (3-propoxy-1, 2-diol) for histone deacetylase inhibitory effect. *Eurasian Chemical Communications*, 2023 5(9), 812-831. **Link:** https://www.echemcom.com/article_171893.html